Thermally Induced Phase Transition of Glucose-Sensitive Core-Shell Microgels

ARTICLE *in* ACS APPLIED MATERIALS & INTERFACES · MARCH 2010

Impact Factor: 6.72 · DOI: 10.1021/am900779a · Source: PubMed

4 AUTHORS, INCLUDING:

Yongjun Zhang
Nankai University
89 PUBLICATIONS **1,780** CITATIONS

SEE PROFILE

ARTICLE

Thermally Induced Phase Transition of Glucose-Sensitive Core−Shell Microgels

Qiaofang Luo, Pengxiao Liu, Ying Guan, and Yongjun Zhang*

Key Laboratory of Functional Polymer Materials, Institute of Polymer Chemistry, College of Chemistry, Nankai University, Tianjin 300071, China

ABSTRACT Four series of poly(*N*-isopropylacrylamide) (PNIPAM) (core)/poly(*N*-isopropylacrylamide-co-3-acrylamidophenylboronic acid) (P(NIPAM-AAPBA)) (shell) microgels were synthesized by the modification of PNIPAM (core)/poly(*N*-isopropylacrylamide-co-acrylic acid) (P(NIPAM-AA)) (shell) microgels with 3-aminophenylboronic acid (APBA). Their thermosensitive behaviors were studied by dynamic light scattering. Two or three phase transitions were detected depending on the shell thickness. These transitions were confirmed by the first derivative plot of the turbidity data. The first transition occurring at about 17 °C was assigned to that of the P(NIPAM-AAPBA) shell, whereas the second and third ones, which occur at about 22 and 28 °C, respectively, were assigned to that of the PNIPAM core. These results indicate that the influences of a shrunk P(NIPAM-AAPBA) shell on the different parts of the PNIPAM core are different. As the outer part, or the "shell" part of the PNIPAM core, directly connects with the P(NIPAM-AAPBA) shell, its phase transition temperature is reduced to a larger degree as compared with that of the inner part, or the "core" part. Glucose-induced swelling was observed for all the microgels, indicating their glucose-sensitivity. However, the degree of glucose-induced swelling is much smaller than that of the pure P(NIPAM-AAPBA) microgels.

KEYWORDS: microgel • core/shell structure • thermosensitive • volume phase transition • poly(*N*-isopropylacrylamide) • glucose sensitive

INTRODUCTION

Microgels are crosslinked spherical hydrogel particles with a diameter ranging from 10 nm to 1000 nm (1, 2). Among them, the thermosensitive poly(*N*-isopropylacrylamide) (PNIPAM) microgels attract considerable attentions in the literature (1, 2). These colloidal particles are highly swollen at low temperature, but undergo sharp volume phase transition at the lower critical solution temperature (LCST) of the PNIPAM polymer (about 32°C). Besides temperature, other external stimuli, such as pH, ionic strength, light (3, 4), and electric field, may also induce deswelling of the microgel particles. Therefore, these intelligent materials have found applications in a wide range of fields such as chemical sensing and biosensing, catalysis, optics (5), separations, and drug delivery (6).

To explore their applications further, more advanced polymer architectures that can lead to materials with superior properties are highly desirable. In this context, Lyon and co-workers first synthesized PNIPAM microgels with core-shell morphologies (7). Since then, a lot of core/shell microgels have been synthesized by Lyon (8−11), Richtering (12) and other authors (13, 14). Most of these works adopted Lyon's method to synthesize core−shell microgels, which is a two-stage free radical precipitation polymerization. Core−shell structure with sharp interface of the resultant microgels was confirmed by TEM (7) and also nonradiative energy transfer measurement (8).

Because the two domains are mechanically linked, it is expected that the degree of swelling of the core and shell regions is mutually influenced (10−12, 15). Lyon et al's results show that the core is restricted from swelling to its native volume in the presence of the shell. With the topological restraints of the shell, the core may undergo phase transition at a temperature lower than its native VPTT (volume phase transition temperature) (10, 11). Similar phenomena were also observed by Richtering et al. (12, 15). Although the VPTT of the two domains may be altered because of their mutual interaction, usually only two phase transitions were observed, which are corresponding to that of the core and the shell, respectively (12, 15). However, Richtering et al. reported that a third peak appears on the differential scanning calorimetry (DSC) thermograms of a PNIPAM (core)/poly-*N*-isopropylmethacrylamide (PNIPMAM) (shell) microgel (16), implying that the mutual interaction between core and shell may result in more complicated thermosensitive behavior of the core/shell microgels.

Previously, we synthesized poly(*N*-isopropylacrylamide-co-3-acrylamidophenylboronic acid) (P(NIPAM-AAPBA)) microgels that display distinct thermosensitive and glucose-sensitive behaviors (17). We believe that this material may find applications for self-regulated insulin delivery (18) and glucose sensing (19, 20). Here, we synthesized a series of core/shell microgels with a PNIPAM core and a P(NIPAM-AAPBA) shell. A core−shell structure is highly desirable for their use as insulin delivery vehicles, in which the PNIPAM core may act as drug reservoir and the P(NIPAM-AAPBA) shell, which should be glucose-sensitive too, may control the rate of drug delivery. In this work, their thermosensitive behaviors were studied by dynamic light scattering and

* To whom correspondence should be addressed. E-mail: yongjunzhang@nankai.edu.cn.

Received for review November 10, 2009 and accepted February 3, 2010

DOI: 10.1021/am900779a

Published on Web 02/12/2010

Table 1. Recipes for the Synthesis of PNIPAM (core)/P(NIPAM-AA) (shell) Microgels with Different Shell Thickness

sample	core solution (mL)	water (mL)	SDS solution (mL)	ahell solution (mL)	0.06M APS (mL)
CxSM1	25	58.75	10	6.25	5
CxSM2	25	52.5	10	12.5	5
CxSM3	25	40	10	25	5

turbidity. Interestingly, a complicated three-stage phase transition was observed for these core−shell microgels.

EXPERIMENTAL SECTION

Materials. *N*-Isopropylacrylamide (NIPAM), *N*,*N*′-methylenebis(acrylamide) (BIS), ammonium persulfate (APS), sodium dodecyl sulfate (SDS), acrylic acid (AA), *N*-(3-dimethylaminopropyl)-*N*′-ethyl-carbodiimide hydrochloride (EDC) are all purchased from Aldrich. 3-aminophenylboronic acid (APBA) and D-(+)-glucose were purchased from ACROS. NIPAM was purified by recrystallization from hexane/acetone mixture and dried in a vacuum. AA was distilled under reduced pressure. Other reagents were used as received.

Microgel Synthesis. Four series of PNIPAM (core)/poly(*N*-isopropylacrylamide-co-acrylic acid) (P(NIPAM-AA)) (shell) microgels were synthesized (11). Each series were synthesized using the same PNIPAM core solution but added a P(NIPAM-AA) shell with different thickness. First, 4 PNIPAM core microgels with various cross-link densities were synthesized. For their synthesis, NIPAM, BIS, and SDS (0.057g) were dissolved in 50 mL of water. The total amount of NIPAM and BIS in feed was all 0.014 mol, whereas their molar ratio, NIPAM:BIS = $(100-x)$:x, was varied to obtain microgels with various cross-link density. The solution was filtered and transferred to a 250 mL, three-necked flask with the help of 150 mL of water. It was purged with N_2 and heated to 70°C. One hour later, 5 mL of 0.06M APS was added to initiate the polymerization. The reaction was allowed to process for 5 h. The resultant microgels were dialysized against water for 1 week to remove impurities. These microgels were denoted as Cx, where x = 1, 2, 5, and 10, indicating the BIS feeding ratio is 1, 2, 5, and 10%, respectively.

PNIPAM (core) / P(NIPAM-AA) (shell) microgels were synthesized by adding a P(NIPAM-AA) shell onto the PNIPAM cores. To control the shell thinkness, various amounts of shell solutions were fed. The stock shell solution was prepared by dissolving 1.400 g of NIPAM, 0.030 g of BIS, and 0.113 g of AA in 100 mL of water. The stock SDS solution was prepared by dissolving 0.570 g of SDS in 100 mL of water. According to the recipes in Table 1, the core solution, SDS solution, and water were added to a flask. The mixture was purged with N_2 and heated to 70°C. Then the preheated shell solution was added. After purging with N_2 for another 30 min, 5 mL of 0.06M APS solution was added to initiate the polymerization. The reaction was allowed to process for 5 h. The resultant microgels were dialysized against water for 1 week to remove impurities. The core/shell microgels were denoted as CxSM1-3, which means they use Cx as the core.

Modification with 3-Aminophenylboronic Acid. APBA (0.233 g; finial concentration, 0.025 M) and 0.239 g of EDC (final concentration, 0.025 M) were dissolved in 45 mL of water that was pre-cooled by ice bath. To the mixture 5 mL of PNIPAM (core)/P(NIPAM-AA) (shell) microgel was added. The reaction mixture was kept at about 0 °C for 4 hours. The resultant products were purified by dialysis against water. The APBA-modified core-shell microgels were labeled as CxSBM1-3, respectively, corresponding to CxSM1-3.

Dynamic Light Scattering. The hydrodynamic radii (R_h) of the microgel particles were measured by dynamic light scattering with a Brookhaven 90Plus laser particle size analyzer. All the measurements were carried out at a scattering angle of 90°. The sample temperature was controlled with a build-in Peltier temperature controller.

Turbidity. The turbidity of the diluted microgel dispersions, which is represented as the absorbance at 550 nm, was measured on a TU-1810PC UV−vis spectrophotometer (Purkinje General, China) using water as reference. Temperature was controlled with a refrigerated circulator.

Other Characterizations. TEM images of the core-shell microgles were acquired with a Philips T20ST transmission electron microscope. The particles were stained by mixing the microgel dispersion with equal amount of 1 mM $Pb(NO_3)_2$. Samples were prepared by applying a drop of the dispersion on Formvar-coated grids which were dried at ambient conditions. Fourier transform infrared (FTIR) spectra were measured on a Bio-Rad FTS-6000 spectrometer. ^{1}H NMR spectra were recorded on a Varian UNITY-plus 400 NMR spectrometer using DMSO-d_6 as solvent.

RESULTS AND DISCUSSION

To synthesize PNIPAM (core)/P(NIPAM-AAPBA) (shell) microgels, we first synthesized microgels with a PNIPAM core and a P(NIPAM-AA) shell according to Lyon et al's method (10). First, a PNIPAM core was synthesized using the radical precipitation polymerization of NIPAM at 70°C, then a P(NIPAM-AA) shell was added to the PNIPAM core. Using this method, 4 series of PNIPAM core and P(NIPAM-AA) shell microgels were synthesized. Each series of microgels used the same PNIPAM core microgel as the core but added various amount of shell solution to obtain P(NIPAM-AA) shells with different thickness. The only difference for each series of core/shell microgels is the crosslink density of the PNIPAM core. BIS feeding ratio is 1, 2, 5, and 10%, respectively. The cross-link density and AA content in the P(NIPAM-AA) shells are all the same. The feeding ratio of BIS and AA is ∼1.5% and ∼10%, respectively. A typical TEM image of the core-shell particles was shown in Figure 1S (see the Supporting Information) in which the P(NIPAM-AA) shell was preferentially stained with Pb^{2+} ions. The image clearly shows a core−shell structure. No solid dark particles were observed, indicating that no homonucleated P(NIPAM-AA) microgels were generated when adding the P(NIPAM-AA) shell.

As an example, Figure 1 compares the volume phase transition behavior of the series of PNIPAM (core)/ P(NIPAM-AA) (shell) microgels with a 2 mol % BIS-crosslinked core at pH3.5. The sizes of the core-shell microgels are bigger than that of its parent core both in the swollen state and the collapsed state. In addition, the overall size increases with increasing shell solution fed. These results confirm again that the P(NIPAM-AA) shells are added onto the PNIPAM core and the shell thickness is controlled by the amount of shell solution fed. All the microgel particles undergo a phase transition at about 30°C, because the VPTT of the P(NIPAM-AA) shell is very close to that of the PNIPAM core at pH 3.5 (pK_a of AA is ∼4.25) (7). From Figure 1, the P(NIPAM-AA) shell in C2SM1 and C2SM2 is very thin. Especially for C2SM1, its size is very close to that of the parent core, C2, at both swollen and collapsed states. In addition, all the microgels exhibit a narrow size distribution with a polydis-

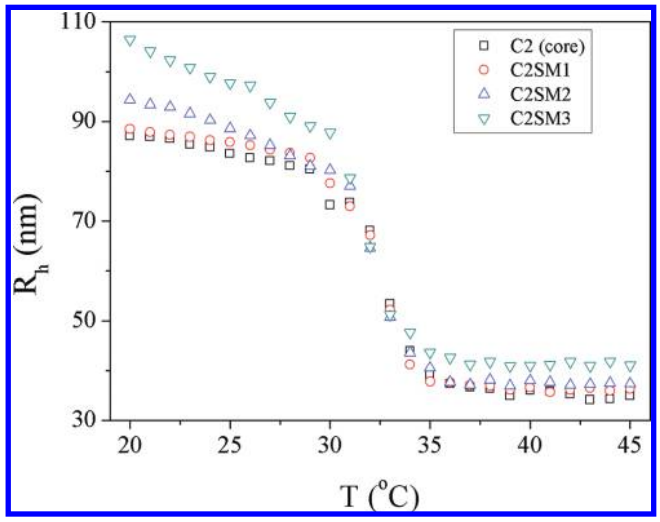

FIGURE 1. Phase transition of the series of PNIPAM (core) / P(NIPAM-AA) (shell) microgels C2SM1-3 and the parent core C2 at pH3.5.

Scheme 1. Conjugation of PBA Groups to the Shell of the Core−Shell Microgel

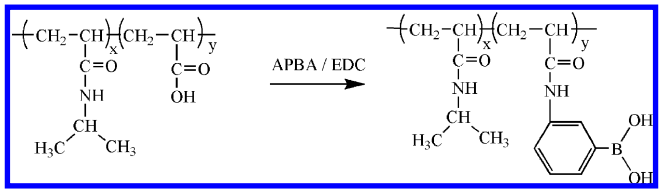

persity below 10%. Upon heating, the measured polydispersity tends to decrease and the size distributions in all cases remain monomodal.

There are three methodologies in the literatures to construct a glucose-sensitive polymer or hydrogel (21), which uses glucose oxidase (GOD), concanavalin (Con A), and phenylboronic acid (PBA) as glucose-sensing moiety, respectively. As in our previous paper, we use PBA as glucose-sensing moiety (17). Compared with the protein-based hydrogels, which are sensitive to environmental changes and have a limited shelf life, the PBA-based hydrogel is totally synthetic and may overcome the problems of stability, toxicity and immunogenicity (22). The PBA groups were introduced by treating the PNIPAM (core)/ P(NIPAM-AA) (shell) microgels with EDC and APBA according to the reaction shown in Scheme 1 (17). To ensure a complete conversion, we used more than 60-fold excess of EDC and APBA.

The resulting microgels have a PNIPAM core and a P(NIPAM-AAPBA) shell. In addition, a P(NIPAM-AAPBA) microgel with the same composition of the shell was synthesized by modification of P(NIPAM-AA) microgel in the same way. The FTIR spetra of the P(NIPAM-AA) microgel before and after modification were shown in Figure 2S (see the Supporting Information). The disappearance of the peak at 1713 cm^{-1} suggestes that the carboxylic groups in the PAA segments are almost completely reacted with APBA. The changes in NMR spectra were shown in Figures 3S and 4S (see the Supporting Information) using DMSO-d6 as solvent. Before modification, the microgel presents peaks at 12.01 and 7.21 ppm that are attributed to the carboxylic acid

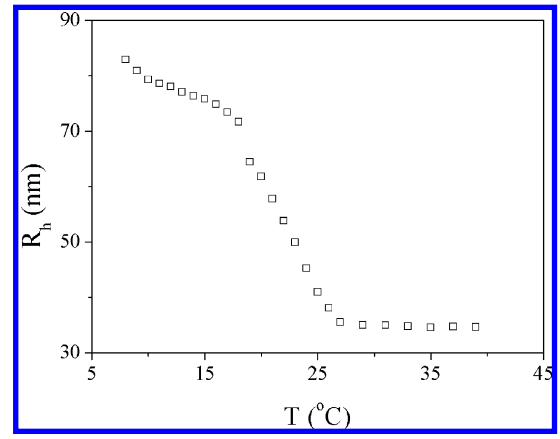

FIGURE 2. Average R_h value of the P(NIPAM-AAPBA) microgel as a function of temperature, measured at pH 3.5 and a scattering angle of 90°.

proton in the PAA segments and the amine proton in the PNIPAM segments. After modification, the peak at 12.01 ppm disappears totally, confirming again an almost completive conversion of the carboxylic acid groups. The new peak at 8.08 ppm (-$B(OH)_2$ proton) and the peaks from 7.05−7.94 ppm (phenyl protons) confirms the successful introduction of PBA groups. These results indicate that an almost complete conversion of the carboxylic acid groups can be achieved by EDC coupling under the experimental conditions.

The thermosensitive behaviors of these core-shell microgels were first studied using dynamic light scattering. The thermosensitive behaviors of the P(NIPAM-AAPBA) microgel and the PNIPAM (core)/P(NIPAM-AAPBA) (shell) microgels were shown in Figures 2 and 3, respectively. From Figure 2, the P(NIPAM-AAPBA) microgel presents a sharp phase transition at about 18 °C. The shift of VPTT to lower temperature compared with the parent P(NIPAM-AA) microgel is attributed to the replacement of the hydrophilic monomer AA with the highly hydrophobic monomer AAPBA (17). On the basis of these observations, we had expected that the PNIPAM (core)/P(NIPAM-AAPBA) (shell) microgels may present distinct two phase transitions, which are corresponding to that of the core and the shell, respectively, because their VPTT difference is as high as 14°C. The results shown in Figure 3 disconfirm our expectation. For each series of microgels, the phase transition profiles of the core-shell microgels deviate from that of the parent core gradually with increasing P(NIPAM-AAPBA) shell thickness. No distinct two-phase transitions were observed. Instead, several small transitions can be detected from the phase transition profiles. Usually for the CxSBM1 mcirogels, two phase transitions can be detected, whereas three phase transitions can be detected for the CxSBM2 and CxSBM3 microgels. The VPTTs, which are defined as the onset of each transition, of the four series of microgels were summarized in Table 2.

Considering the small extent of these transitions and the fluctuation and relatively big experimental errors of the R_h data from light scattering (23), the determination of these transitions is somewhat arbitrary. Turbidity is another commonly-used method to study the phase transition of PNIPAM microgels. Because the refractive index of the microgel

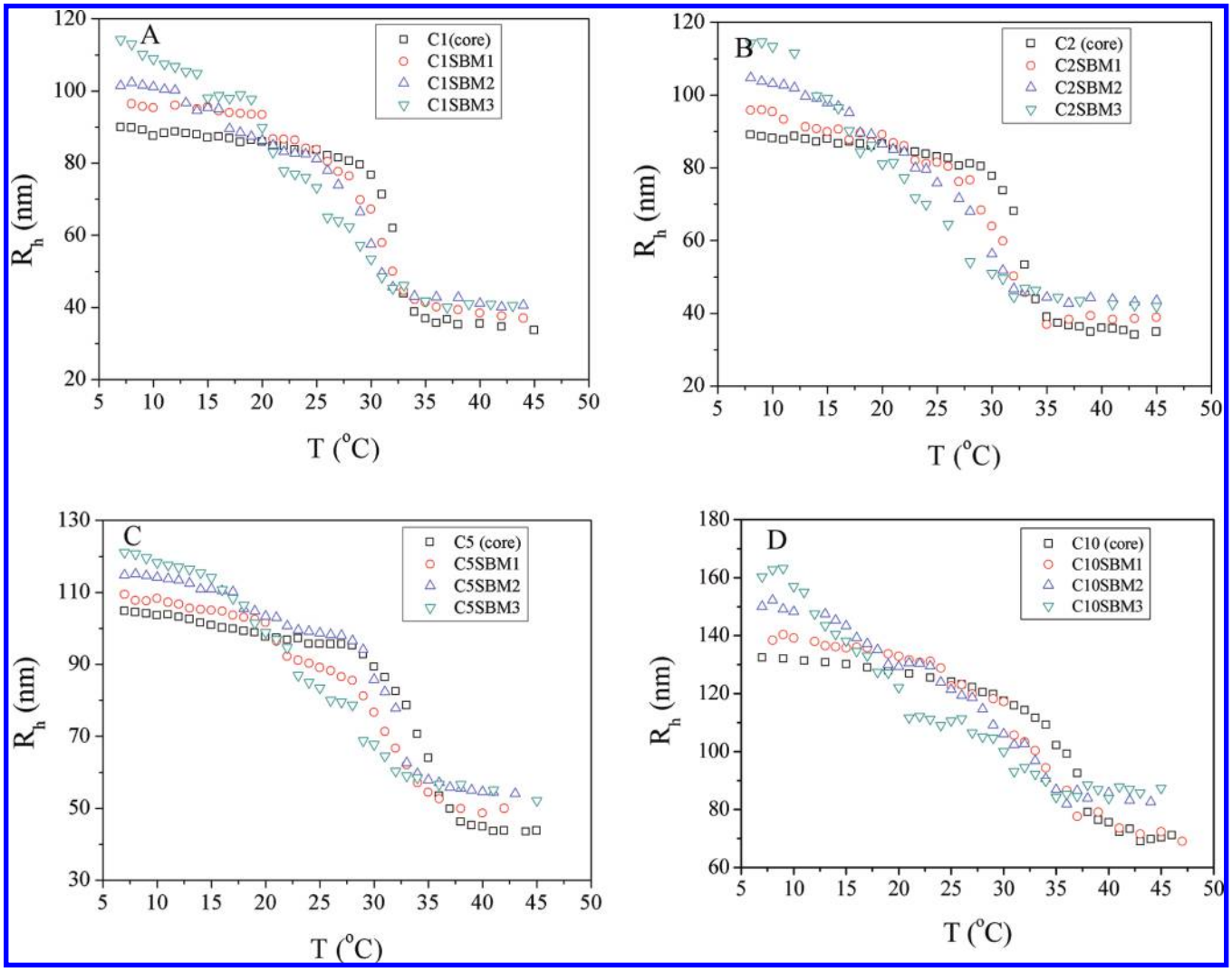

FIGURE 3. Average R_h value of the PNIPAM (core) / P(NIPAM-AAPBA) (shell) microgels as a function of temperature, measured at pH 3.5 and a scattering angle of 90°. (A) C1 and C1SBM1-3. (B) C2 and C2SBM1-3. (C) C5 and C5SBM1-3. (D) C10 and C10SBM1-3. The uncertainty of the data is around 3%.

Table 2. Volume Phase Transition Temperatures (VPTT) of the Core−Shell Microgels and the Parent Core Microgels Detected by Dynamic Light Scattering

	VPTT (°C)			
BIS content in the core (x %)	Cx (core)	CxSBM1	CxSBM2	CxSBM3
1	30	20,28	16, 21, 26	14, 19, 25
2	30	22,28	17, 22, 28	16, 21, 26
5	30	20,28	17, 21, 29	15, 22, 28
10	34	24,30	15, 23, 32	17, 20, 29

sphere increases as the sphere deswells (24), a sharp increase in turbidity can be observed when a phase transition occurs. As a method to study phase transition of PNIPAM microgels, the turbidity method has the advantage that the turbidity of a microgel dispersion can be measured with high precision and repeatability.

The turbidity data for the core microgels and also P(NIPAM-AAPBA) microgel were plotted in Figure 4A. The corresponding first derivative plots were shown in Figure 4B. All the microgels undergo sharp deswelling at VPTT, which results in sharp increase in turbidity. The first derivative plot of the turbidity data presents a symmetrical peak. These results imply that a peak on the first derivative plot may represent a phase transition, and the peak temperature can be regarded as the temperature of the phase transition (25). From Figure 4B, VPTT were determined to be 32.7, 33.7, 33.7, and 37.7 °C for the four core particles with BIS feeding ratio of 1, 2, 5, and 10%, respectively. The increasing VPTT with increasing crosslink density can be attributed to the shorter subchains in the microgels (26). The VPTT for P(NIPAM-AAPBA) from Figure 4B is 23 °C. Note that the VPTT data are different from that obtained from dynamic light scattering because of their different definition. In dynamic light scattering, VPTT is defined as the onset of phase transition, whereas in turbidity, VPTT is actually the midpoint of the phase transition process. Usually the VPTT determined by turbidity is larger than the one by light scattering. The difference between them depends on the extent of the transition.

Figure 5 shows the turbidity data for the series of core/shell microgels with 1 mol % BIS- crosslinked core, i.e.,

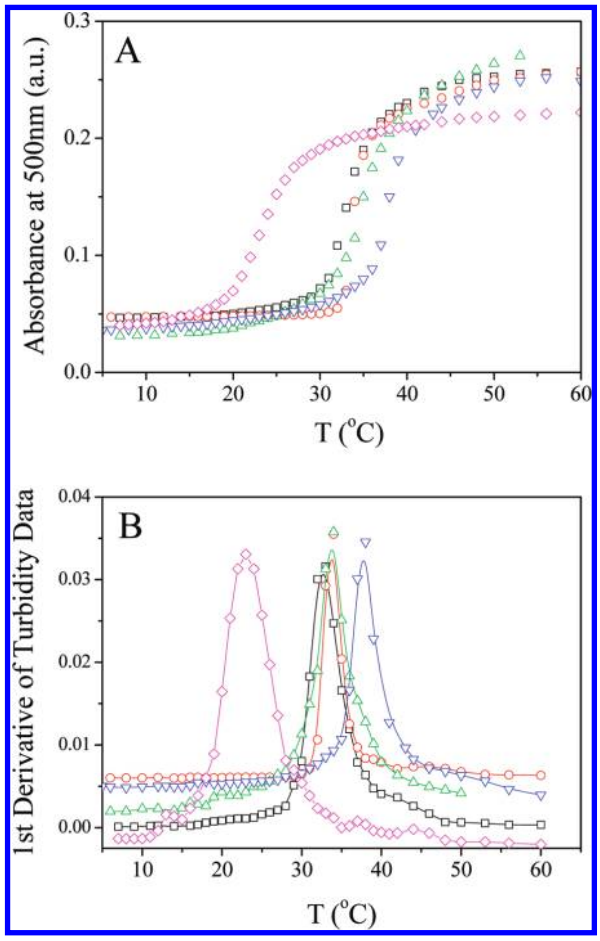

FIGURE 4. (A) Turbidity as a function of temperature for the core microgels (□, C1; ○, C2; △, C5; and ▽, C10) and P(NIPAM-AAPBA) microgel (◇). (B) First derivative plot of the turbidity data.

C1SBM1-3 microgels. For comparison, the corresponding light scattering data were plotted on the same figure. From the turbidity data, the core microgel C1 undergoes only one phase transition at about 33 °C. C1SBM1 with the thinnest P(NIPAM-AAPBA) shell presents two phase transitions at 26 and 32 °C, respectively. Both C1SBM2 and C1SBM3, with thicker P(NIPAM-AAPBA) shells, present three phase transitions. The transitions occur at 17, 24, and 31 °C for the former and 18, 24, and 29 °C for the latter. These results are in agreement with the light scattering data. Each transition detected from turbidity can find a corresponding transition from the R_h−T plot, confirming the occurrence of these transitions.

The above observation reveals that the PNIPAM (core)/P(NIPAM-AAPBA) (shell) microgel particles undergo a three-stage phase transition upon heating. The first transition occurs at about 17 °C, which is close to the VPTT of pure P(NIPAM-AAPBA) microgels, so it can be attributed to the deswelling of the P(NIPAM-AAPBA) shell. This transition was not detectible for C1SBM1, because its P(NIPAM-AAPBA) shell is the thinnest among the three core−shell particles. In contrast, it was detected for both C1SBM2 and C1SBM3 because of their increased shell thickness, which makes its transition detectible. The other two transitions occur at about 24 and 31 °C, respectively.

Previously, Richtering et al. observed a third peak on the DSC thermogram of a PNIPAM (core)/PNIPMAM (shell) microgel besides other two peaks corresponding to the transition of core and shell. This transition was only observed for the core/shell particle with the thickest shell. The authors suggested that the additional thermal transition is caused by the breaking of hydrogen bonds between mechanically stretched chain segments. They hypothesized that the altered chain conformations lead to the formation of different hydrogen bonds, the breaking of which leads to the additional thermal transition. It is not clear how the "different" hydrogen bonds form in the core−shell microgels. In addition, the explanation can not answer why these different hydrogen bonds form only in microgels with the thickest shell.

Here we propose that the three-stage transition can be explained by the heterogeneous structure of the PNIPAM microgels. Several groups have shown that the crosslink density (i.e., BIS content) decreases gradually from the core towards the periphery because the cross-linking monomer BIS has a higher polymerization rate than the PNIPAM monomer (27−30). The heterogeneous structure of a PNIPAM microgel can be described as a quasi-core−shell-like structure with a "core" with a higher cross-link density and a "shell" with a lower cross-link density. The phase transition temperature of PNIPAM chains depends on the length of the subchain between two neighboring cross-linking points (26). Therefore the phase transition temperature of the "shell", which has a lower cross-link density, should be lower than that of the "core". However, the difference between the two VPTTs is so small that only one transition will be observed for common PNIPAM microgels.

The PNIPAM cores in the core/shell particles should also present a core−shell-like heterogenous structure as illustrated in Scheme 2. In the absence of the P(NIPAM-AAPBA) shell, VPTT of the "core" is just slightly higher than that of the "shell"; however, the VPTT difference is increased by the addition of a P(NIPAM-AAPBA) shell. As a result, two phase transitions can be observed (i.e., the second and the third transition in the core−shell microgels). The P(NIPAM-AAPBA) shell can influence the VPTT of the "shell" (the outer part of the PNIPAM core) in two ways. First, the shrinkage of the P(NIPAM-AAPBA) shell applies mechanical pressure directly on the "shell", which will facilitate its collapse. Secondly, the shrunk, hydrophobic P(NIPAM-AAPBA) shell, to which the "shell" conjugates directly, should alter its hydrophilic/hydrophobic balance, therefore reduces its phase transition temperature. It is well known that the phase transition temperature of PNIPAM will considerably decrease when capped with hydrophobic terminal groups (31). Both effects lead to a lower VPTT of the "shell". On the opposite, because the "core" (the inner part of the PNIPAM core) is separated from the shrunk P(NIPAM-AAPBA) shell, its effect on the "core" will be much smaller. As a result, the difference in VPTT between the "core" and "shell" is increased.

Previously, Lyon et al. studied the phase transition of a core−shell microgel with a PNIPAM core and a P(NIPAM-

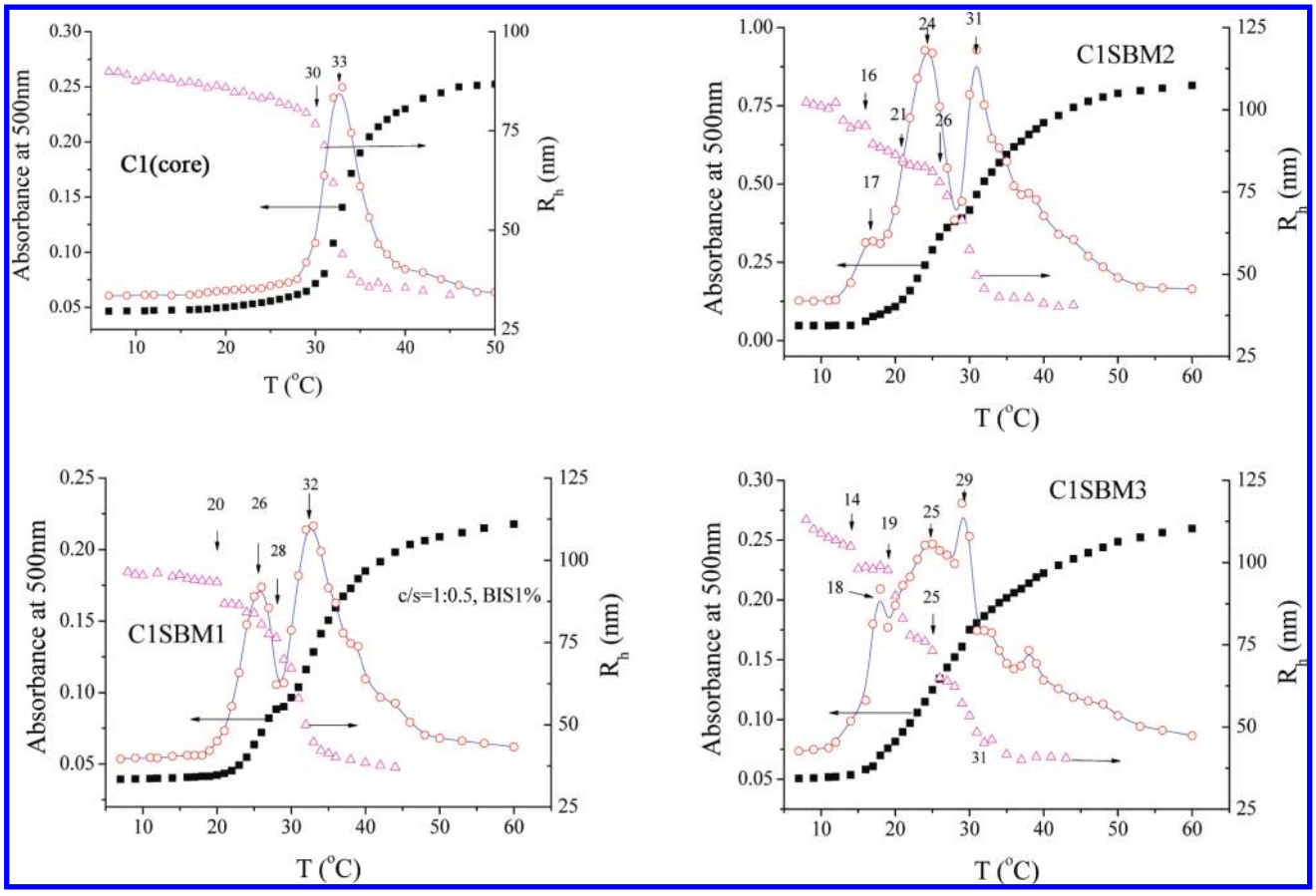

FIGURE 5. Turbidity data as a function temperature for microgels C1 and C1SBM1-3 (■) and the corresponding first derivative plot of the turbidity data (○). R_h data (Δ) are also included for comparison. The VPTT values were labeled.

Scheme 2. Schematic Illustration of the Structure of PNIPAM (core)/P(NIPAM-AAPBA) (shell) Microgel Particles; The PNIPAM Core Can Be Further Divided as a BIS-Rich, Highly Cross-Linked "Core" and a BIS-Poor, Lightly Cross-Linked "Shell"

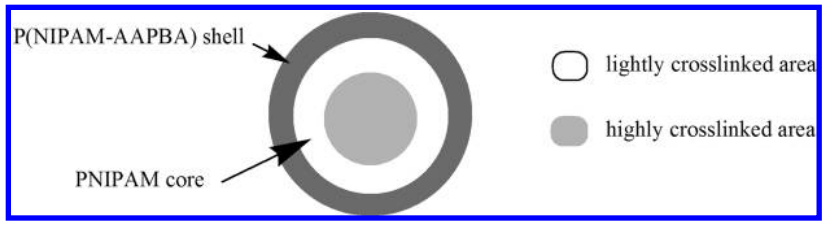

AA) shell at pH 6.5 (7). As the carboxylic acid groups deprotonate at this pH, the VPTT of P(NIPAM-AA) microgel with the similar composition is as high as 60 °C. However, for the PNIPAM (core)/P(NIPAM-AA) (shell) microgel, several phase transitions were observed below 60 °C. These transitions was attributed to various P(NIPAM-AA) shell areas that couple with the PNIPAM core to a various extent and thus depressed VPTT to various extent. On the opposite, here we show because the various core areas couple with a shell to a various extent, they present depressed VPTT to various extent.

Other effects of the P(NIPAM-AAPBA) shell on the deswelling of the PNIPAM core were also detected. Lyon et al. reported that a shrunk shell restrains the core from fully swelling. As a result, the overall size of the core/shell particle can be smaller than its parent core at an intermediate range of temperature (11). Similar phenomena were also observed for our CxSBM microgels. (Figure 3) In addition, because the PNIPAM core is compressed by a shrunk shell, its VPTT (both "shell" and "core" parts) is lower than that of a native PNIPAM microgel.

Recently, Lapeyre et al synthesized similar core/shell microgels with PNIPAM as core and P(NIPAM-AAPBA) as shell (32); however, the thermal behaviors of their microgels is totally different from the ones reported here. The reason should be attributed to the different synthetic method which results in different microstructure. Lapeyre et al synthesized the P(NIPAM-AAPBA) shell by direct copolymerization of NIPAM and AAPBA, while we synthesized it via the modification of a parent P(NIPAM-AA) shell with APBA under EDC catalysis, as shown in Scheme 1. As Hoare et al. (33, 34) demonstrated, the radial and intrachain distributions of functional groups within the 3D microgel network are very different when NIPAM copolymerizes with different comono-

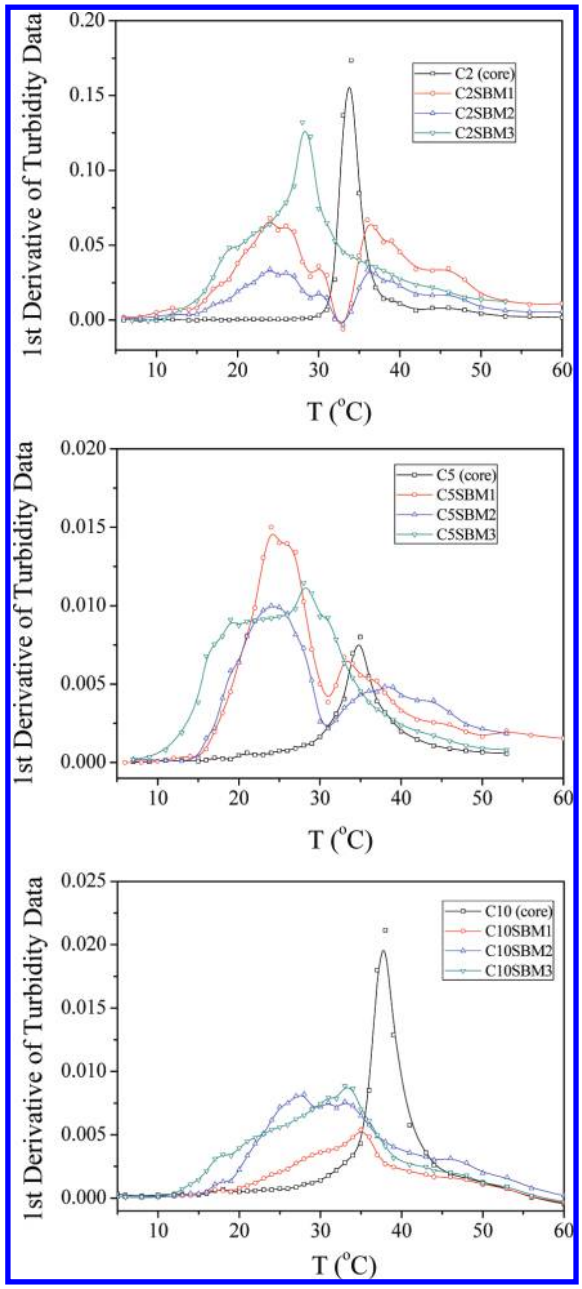

FIGURE 6. First derivative plot of the turbidity data for the series of core/shell microgels with a core BIS content of 2, 5, and 10%, respectively.

mers, which in turn significantly influence the behavior of the resulting microgel. According to Hoare et al., P(NIPAM-AA) microgels (or shells) have a relatively even distribution of functional groups (33), as do the P(NIPAM-AAPBA) microgels or shells derived from them. In contrast, P(NIPAM-AAPBA) microgels or shells by direct copolymerization may present complicated heterogenous microstructures because of the different reaction rate of NIPAM and AAPBA.

The first derivative plot of turbidity data for other series of core/shell microgels were shown in Figure 6. As compared with the series with a core crosslink density of 1%, more peaks or shoulders present in these plots. These peaks or shoulders can still be explained by the three transitions we proposed above. For example, on the plot of C2SBM1, there exist 5 peaks (or shoulders) at about 17, 21, 24, 26, and 30 °C, respectively. The three ones at 17, 24, and 30 °C and can be assigned to the three phase transitions we proposed above, respectively. The other two peaks can be assigned as a combined result of the neighbor transitions. It is very likely that at these intermediate temperatures, although the increased rate of turbidity caused by the first transition begins to decline, the onset of the second transition results in an enhanced turbidity increase. As a combined result of the two opposite effects, an additional peak or shoulder appears at these intermediate temperatures.

Scheme 3. Complexation Equilibrium between Phenylboronic Acid Derivative and Glucose

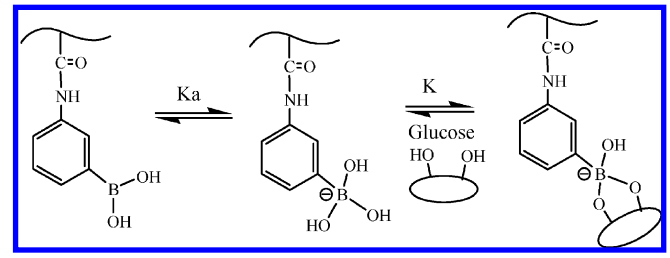

The principle for PBA group using as glucose sensing moiety was shown in Scheme 3. The binding of PBA groups with glucose converts more PBA groups from the neutral, hydrophobic form to negatively charged, hydrophilic form. For a hydrogel modified with PBA group, the binding of diols increases the degree of ionization on the hydrogel and builds up a Donnan potential for its swelling. We have shown the P(NIPAM-AAPBA) microgel swells to a larger degree in the presence of glucose (17). The PNIPAM (core) / P(NIPAM-AAPBA) (shell) microgels synthesized here present similar glucose-sensitive behaviors. Figure 7 shows the glucose-induced swelling of C1SBM1-3 microgels. The ratio of the particle size at [Glu] = 0.1 M to that in the absence of glucose ($R_{h,0.1M}/R_{h,0}$) was calculated to be 1.19, 1.26, and 1.37, for C1SBM1-3, respectively, indicating that the glucose-induced swelling increases with increasing P(NIPAM-AAPBA) shell thickness. Other series of microgels present the same trend (Table 3). It seems that the cross-link density in the core does not significantly influence the degree of glucose-induced swelling. Compared with the pure P(NIPAM-AAPBA) micro-

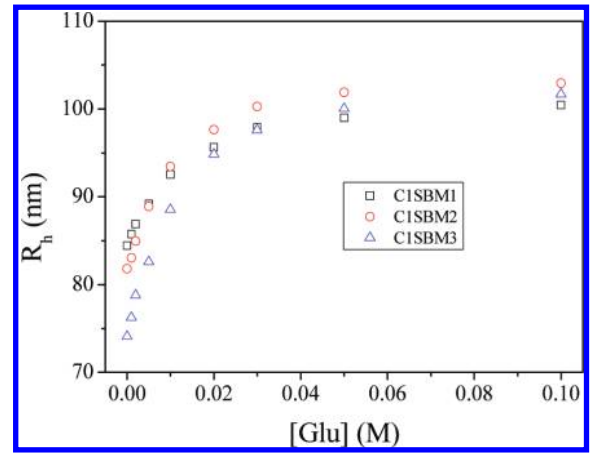

FIGURE 7. Glucose-induced swelling of C1SBM1-3 microgels. Measured in 5 mM pH8.5 phosphate buffer at 25°C. The scattering angle is 90°.

Table 3. Ratio of R_h at [Glu] = 0.1 M to That in the Absence of Glucose ($R_{h,0.1M}/R_{h,0}$) of the 4 Series of Core–Shell Particles

	$R_{h,0.1M}/R_{h,0}$		
BIS content in the core (x%)	CxSBM1	CxSBM2	CxSBM3
1	1.19	1.26	1.37
2	1.22	1.29	1.37
5	1.19	1.21	1.26
10	1.19	1.22	1.3

gel we prepared previously (17), which swells to two-fold of its original size in the presence of glucose, the glucose-induced swelling of the core–shell particles is smaller. This result is reasonable, considering only the shell contains glucose-responsive groups.

In conclusion, four series of core–shell microgels with a PNIPAM core and a P(NIPAM-AAPBA) shell were synthesized by the modification of the PNIPAM (core)/P(NIPAM-AA) (shell) microgels with APBA. Their thermosensitive behaviors were studied by dynamic light scattering and turbidity. When heating, these core–shell microgels experience three phase transitions. The first one is assigned to that of the P(NIPAM-AAPBA) shell, whereas the second and the third are assigned to that of the PNIPAM core. The appearance of two transitions of the PNIPAM core was explained by its core–shell-like heterogeneous structure and the different effect of the P(NIPAM-AAPBA) shell on them. The "shell" part of the PNIPAM core directly connects with the shrunk, hydrophobic P(NIPAM-AAPBA) shell; therefore, its VPTT is lowered to a larger extent than that of the "core" part. The VPTT difference between the two parts is increased by the P(NIPAM-AAPBA) shell, resulting in two transitions on its deswelling profile. These core–shell particles also swell in the presence of glucose; however, the degree of the glucose-induced swelling is smaller than that of the pure P(NIPAM-AAPBA) microgels.

Acknowledgment. We are grateful for financial support for this work from the National Natural Science Foundation of China (Grant 20774049), Ministry of Science and Technology of China (Grant 2007DFA50760), and Tianjin Committee of Science and Technology (07ZCGHHZ01200).

Supporting Information Available: TEM image of C5SM3 microgel with a PNIPAM core and a P(NIPAM-AA) shell, FTIR and NMR spectra of P(NIPAM-AA) microgel before and after EDC coupling with 3-aminophenylboronic acid (PDF). This material is available free of charge via the Internet at http://pubs.acs.org.

REFERENCES AND NOTES

(1) Pelton, R. *Adv. Colloid Interface Sci.* **2000**, *85*, 1–33.
(2) Saunders, B. R.; Vincent, B. *Adv. Colloid Interface Sci.* **1999**, *80*, 1–25.
(3) Nayak, S.; Lyon, L. A. *Chem. Mater.* **2004**, *16*, 2623–2627.
(4) Gorelikov, I.; Field, L.M.; Kumacheva, E. *J. Am. Chem. Soc.* **2004**, *126*, 15938–15939.
(5) Reese, C. E.; Mikhonin, A. V.; Kamenjicki, M.; Tikhonov, A.; Asher, S. A. *J. Am. Chem. Soc.* **2004**, *126*, 1493–1496.
(6) Das, M.; Mardyani, S.; Chan, W. C. W.; Kumacheva, E. *Adv. Mater.* **2006**, *18*, 80–83.
(7) Jones, C. D.; Lyon, L. A. *Macromolecules* **2000**, *33*, 8301–8306.
(8) Gan, D. J.; Lyon, L. A. *J. Am. Chem. Soc.* **2001**, *123*, 8203–8209.
(9) Gan, D. J.; Lyon, L. A. *J. Am. Chem. Soc.* **2001**, *123*, 7511–7517.
(10) Jones, C. D.; Lyon, L. A. *Langmuir* **2003**, *19*, 4544–4547.
(11) Jones, C. D.; Lyon, L. A. *Macromolecules* **2003**, *36*, 1988–1993.
(12) Berndt, I.; Richtering, W. *Macromolecules* **2003**, *36*, 8780–8785.
(13) Leung, M. F.; Zhu, J. M.; Harris, F. W.; Li, P. *Macromol. Rapid Commun.* **2004**, *25*, 1819–1823.
(14) Chi, C.; Cai, T.; Hu, Z. *Langmuir* **2009**, *25*, 3814–3819.
(15) Berndt, I.; Pedersen, J. S.; Richtering, W. *J. Am. Chem. Soc.* **2005**, *127*, 9372–9373.
(16) Berndt, I.; Popescu, C.; Wortmann, F. J.; Richtering, W. *Angew. Chem., Int. Ed.* **2006**, *45*, 1081–1085.
(17) Zhang, Y.; Guan, Y.; Zhou, S *Biomacromolecules* **2006**, *7*, 3196–3201.
(18) Zhang, Y.; Guan, Y.; Zhou, S *Biomacromolecules* **2007**, *8*, 3842–3847.
(19) Liu, Y.; Zhang, Y.; Guan, Y. *Chem. Commun.* **2009**, 1867–1869.
(20) Wu, W. T.; Zhou, T.; Shen, J.; Zhou, S. *Chem. Commun.* **2009**, 4390–4392.
(21) Matsumoto, A.; Yoshida, R.; Kataoka, K. *Biomacromolecules* **2004**, *5*, 1038–1045.
(22) Kataoka, K.; Miyazaki, H.; Bunya, M.; Okano, T.; Sakurai, Y. *J. Am. Chem. Soc.* **1998**, *120*, 12694–12695.
(23) Takahashi, K.; Kato, H.; Saito, T.; Matsuyama, S.; Kinugasa, S. *Part. Part. Syst. Charact.* **2008**, *25*, 31–38.
(24) Weissman, J. M.; Sunkara, H. B.; Tse, A. S.; Asher, S. A. *Science* **1996**, *274*, 959–960.
(25) Benee, L. S.; Snowden, M. J.; Chowdhry, B. Z. *Langmuir* **2002**, *18*, 6025–6030.
(26) Wu, C.; Zhou, S. *Macromolecules* **1997**, *30*, 574–576.
(27) Varga, I.; Gilanyi, T.; Meszaros, R.; Filipcsei, G.; Zrinyi, M. *J. Phys. Chem. B* **2001**, *105*, 9071–9076.
(28) Wu, X.; Pelton, R. H.; Hamielec, A. E.; Woods, D. R.; McPhee, W. *Colloid Polym. Sci.* **1994**, *272*, 467–477.
(29) Saunders, B. R. *Langmuir* **2004**, *20*, 3925–3932.
(30) Daly, E.; Saunders, B. R. *Phys. Chem. Chem. Phys.* **2000**, *2*, 3187–3193.
(31) Xu, J.; Liu, S. Y. *J. Polym. Sci., Polym. Chem.* **2009**, *47*, 404–419.
(32) Lapeyre, V.; Ancla, C.; Catargi, B.; Ravaine, V. *J. Colloid Interface Sci.* **2008**, *327*, 316–323.
(33) Hoare, T.; McLean, D. *J. Phys. Chem. B* **2006**, *110*, 20327–20336.
(34) Hoare, T.; Pelton, R. *Langmuir* **2008**, *24*, 1005–1012.

AM900779A